

Gradiometers Based on Superconducting Quantum Interference Device for Nondestructive Testing

Yu. V. Maslennikov^{a, b}, V. Yu. Slobodchikov^{a, b}, V. A. Krymov^{a, b}, V. V. Khanin^{a, b}, and V. P. Koshelets^{a, *}

^a*Kotel'nikov Institute of Radio Engineering and Electronics, Russian Academy of Sciences, Moscow, 125009 Russia*

^b*NPO Krioton, Troitsk, Moscow, 101000 Russia*

**e-mail: valery@hitech.cplire.ru*

Received March 30, 2016

Abstract—A prototype of gradiometer for detection and analysis of magnetic signals that are generated by defects in metal structures and materials in the presence of external magnetic bias is based on dc-current superconducting quantum interference device (SQUID). A prototype of single-channel SQUID gradiometer that contains a fiberglass nonmagnetic cryostat, measurement probe with the SQUID sensor and magnetic flux transformer (second-order axial gradiometer), SQUID electronics, and software for control of SQUID gradiometer is studied. The prototype exhibits stable operation under laboratory conditions in the absence of additional magnetic shielding. Upgrade of the SQUID sensors and remaining elements of the prototype of magnetometer is planned for application in nondestructive testing.

DOI: 10.1134/S1064226916120172

INTRODUCTION

Nondestructive testing (NDT) is used for detection, localization, and evaluation of defects in materials and purchased items. Defects can be formed in the course of manufacturing or result from stress and corrosion under real working conditions. Evidently, the methods for detection of critical defects are extremely important for manufacturing and quality testing of working items, quality testing in the course of production, and analysis of malfunctioning. An NDT method can be based on the analysis of eddy currents in the conducting samples under study. However, a disadvantage of the eddy-current method is related to the fact that it can be used only up to certain depths under the surface of the samples under study and cannot be employed for the detection of deep defects. Such limitations can be eliminated with the aid of NDT systems based on high-sensitivity SQUID magnetometers.

The results of successful applications of the NDT systems based on magnetometric SQUID systems in monitoring of materials and structures over the last thirty years have been analyzed in [1]. The advantages of the NDT SQUID systems in comparison with alternative devices are related to high sensitivity (10–100 fT/Hz^{1/2}), wide passband (from zero to several tens of kilohertz), and wide dynamic range (more than 120 dB). The disadvantages of such systems are related to the operation at cryogenic temperatures and, hence, expensiveness of routine measurements. In spite of relatively high price of cryogenic equipment and technical difficulties, the SQUID systems are

employed when the needed efficiency cannot be reached using alternative NDT techniques [2]. The NDT SQUID systems are developed and employed for the detection of defects in steel plates [3], study of stress–strain states in ferromagnetic materials [4], detection of ruptures in steel ropes of bridge structures [5], and detection of cracks in turbine blades of aircraft engines [6].

Extremely high sensitivity of SQUID magnetometers of up to 5 fT/Hz^{1/2} remains unchanged to frequencies of about 1 Hz, so that the SQUID sensors can be used for the detection of deep undersurface defects in conducting materials due to a decrease in the frequency of the excitation eddy currents and a corresponding increase in the thickness of the skin layer. The NDT SQUID systems based on the eddy-current method can be used to detect deep undersurface defects in thick multilayer aluminum structures in aircraft manufacturing.

The purpose of this work is the construction of a prototype of a single-channel SQUID system for applications in NDT systems and the study of the parameters of such a prototype.

1. EQUIPMENT AND METHODS

1.1. SQUID Sensor for the Prototype of Single-Channel SQUID Gradiometer and Its Main Characteristics

SQUID sensor is a key element of the magnetometric system that determines the requirements to the remaining components. We have analyzed the pub-

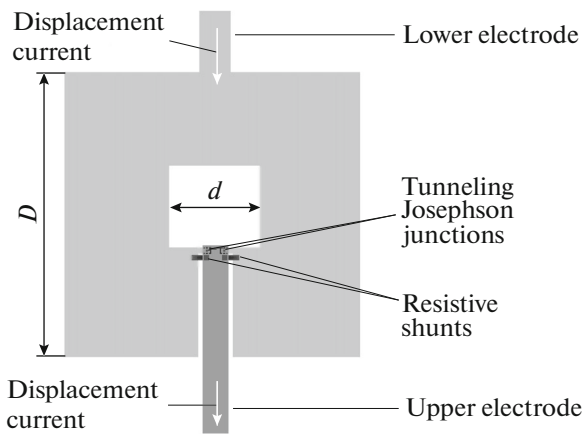


Fig. 1. Topological scheme of the dc-current SQUID that is used in the measurement probe of the prototype of the single-channel NDT system.

lished data on the dc-current SQUIDs that are appropriate for practical application in the nondestructive testing of defects in various materials. We have analyzed both physical characteristics and technological possibilities for small-scale production needed for the development of multichannel magnetometers.

Note that only foreign-made SQUID sensors (SUPRACON AG (Germany) and Star Cryoelectronics (USA)) are commercially available. To develop domestic technologies of superconducting microelectronics and provide import substitution, we use experimental dc-current SQUID devices produced at the Kotel'nikov Institute of Radio Engineering and Electronics [7–9] that can be improved for applications in the NDT magnetometric SQUID systems.

At the first stage, we employ hybrid SQUID sensors in the prototype of the SQUID gradiometer. In such SQUID sensors, the interferometer with the Josephson junctions is fabricated using the thin-film technology and the input coil represents a plane helix containing 20–30 turns of insulated niobium wire that is placed on top of the SQUID interferometer. The external feedback coil represents a single turn with a diameter of 2 mm made of a copper wire with a cross section of 0.1 mm that is placed under the SQUID chip. The main problem of the hybrid SQUID sensors is to realize reasonably large coupling coefficient of the input coil and SQUID interferometer in order to decrease loss of the input signal.

For the solution of the above problem, we use a modification of the SQUID interferometer (Fig. 1) that has been proposed in [10]. The SQUID interferometer contains a square superconducting concentrator of magnetic flux with an external dimension of $D = 2.4$ mm and a central square hole with a size of $d = 0.07$ mm. Two shunted Josephson junctions are placed on the internal contour of the concentrator, and the

upper electrode of the thin-film structure passes through the slots of the interferometer contour.

The chips with such SQUIDs are manufactured at the Kotel'nikov Institute of Radio Engineering and Electronics using the thin-film technology of superconducting microelectronics. The SQUID employs Nb/Al₂O₃/Nb tunneling Josephson junctions with a size of 3×3 μm and a critical current of 15–25 μA . For shunting, we use thin-film molybdenum (Mo) or titanium (Ti) resistors with a resistance of 2–4 Ω . The intrinsic inductance of the SQUIDs is about 120 pH and the range of the signal characteristic is 20–30 μV . The level of intrinsic noise with respect to the magnetic flux is about $3.0 \mu\Phi_0/\text{Hz}^{1/2}$ (here, $\Phi_0 \approx 2.06 \times 10^{-15}$ Wb is the quantum of magnetic flux). Such parameters make it possible to construct prototypes of high-sensitivity SQUID magnetometers for applications in the NDT systems.

Each input coil for the SQUID sensor is manually wound using special equipment the main elements of which are thin axis with a diameter of 0.35 mm made of hard instrumental steel and a rotating device that allow simultaneous winding of two ends of niobium wire in opposite directions with a certain strength. The niobium-wire helix is wound in a gap between Teflon plates that are placed on the axis and fixed due to the force of friction. The gap between the plates (about 0.1 mm) determines the thickness of the spiral input coil. A drop of a BF-4 liquid glue is deposited in the course of winding in the gap between the plates. After winding of the needed number of turns over time interval of no longer than 1 min, the structure is dried and, then, detached from axis of the winding device together with the Teflon plates. Then, the plates are detached using a scalpel or razor blade and the input coil is ready for use.

The SQUID chip is glued on a fiberglass substrate with preliminary glued turn of the feedback coil. The input coil is fixed on top of the SQUID chip with certain mobility using three or four turns of an elastic synthetic yarn around the substrate. The mutual position of the central hole of the SQUID and the hole of the spiral input coil is monitored and adjusted with the aid of a microscope. Then, the yarn is tightened and glued on the opposite side of the substrate.

To provide the superconducting contact of the magnetic flux transformer (second-order axial gradiometer) and input coil, we glue terminals in the substrate that represent two lamellas with a size of 2×5 mm made of niobium foil with a thickness of 0.5 mm. Two M1-thread holes provide mechanical fixing of the gradiometer and input-coil ends. Cleared ends of the gradiometer and input coil are pressed to the glued lamellas using four M1 screws and two movable lamellas made of niobium foil with threadless holes with a diameter of 1 mm.

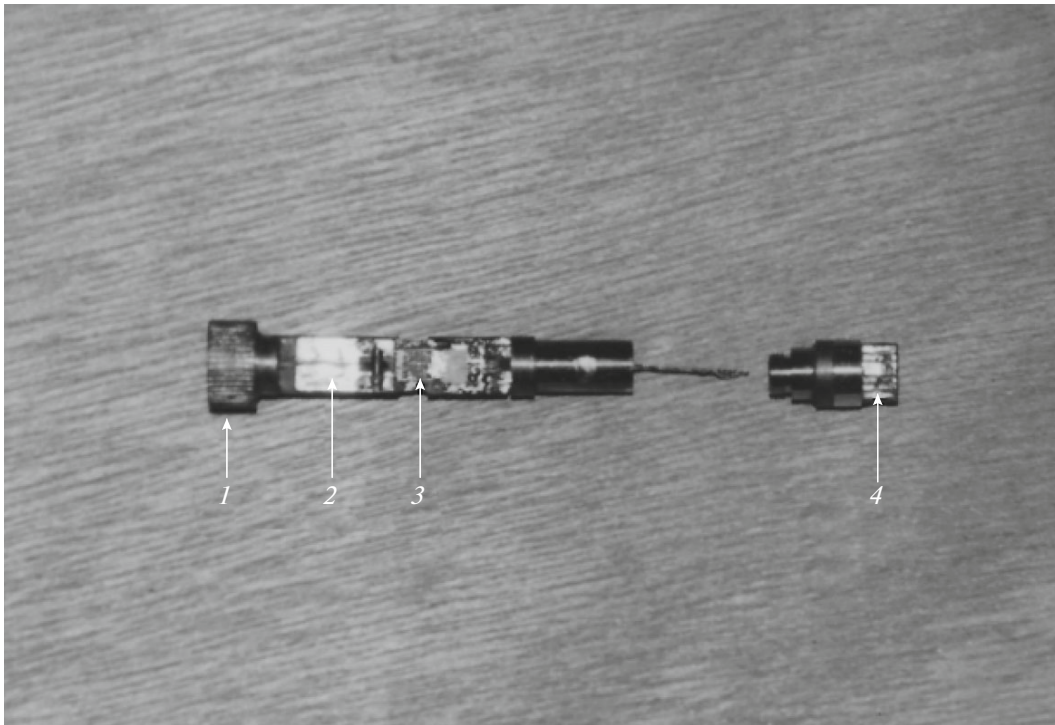


Fig. 2. Photograph of the inner structure of the SQUID sensor for the measurement probe of the prototype of the single-channel NDT system (in the absence of external shields): (1) niobium housing of the SQUID sensor, (2) niobium lamellas for fixing of the niobium-wire ends of the input coil and gradiometer, (3) thin-film SQUID with the input coil on top, (4) output connector.

The SQUID sensor in the prototype of the single-channel NDT system is fabricated as a capsule with double superconducting screen made of niobium tubes with external diameters of 10 and 6 mm containing the dc-current SQUID and the input coil of the flux transformer (Fig. 2).

The SQUID independently works as a high-sensitivity magnetometer, since the SQUID interferometer represents a conventional superconducting film loop. The experimentally measured intrinsic resolution with respect to magnetic field is better than $100 \text{ fT/Hz}^{1/2}$. For the protection against external magnetic fields, we employ a structure that consists of two cylindrical superconducting screens. The first screen with the smaller diameter covers the substrate region with the SQUID chip and input coil. The second screen protects the lamellae region, where the gradiometer and input-coil ends are fixed. The end surfaces of the sensor screens are also covered by niobium items and have small holes with a diameter of 0.5 mm for the end of the twisted pair of gradiometer on the one side and the feedback coil on the opposite side.

Experiments are performed to determine the configuration of spiral with the maximum coupling coefficient with the SQUID interferometer. For this purpose, we use several spiral input coils with 10, 20, and 30 turns. For each coil, we preliminarily measure the inductance at liquid-helium temperature. The spiral coils are mounted on the SQUID chip using the above

procedure. Then, a twisted pair made of copper wire is connected via two 100-k Ω resistors instead of the gradiometer to the input terminals of the SQUID sensor. A test signal of a low-frequency oscillator with a frequency of 8–10 Hz is fed to the SQUID input coil via the twisted pair. The SQUID sensor with the connected circuit of the test signal is fixed on a probe for the study of the SQUID characteristics at working temperature. The probe is connected to magnetometer electronics, and the signal characteristic of the SQUID is observed using an oscilloscope in the regime of the open feedback. Under a variation in the output voltage of the oscillator, a test signal that corresponds to a single quantum of magnetic flux in the SQUID is fed to the input coil. The division of the measured output voltage of the oscillator by the resistance of the circuit (200 k Ω) yields the main parameter of the SQUID sensor, which is coefficient $K_{A-\Phi}$ of the conversion of input current into SQUID magnetic flux (i.e., the current in the input coil that generates a single quantum of the SQUID magnetic flux). We must determine the configuration of the spiral input coil that provides the minimization of the coefficient (i.e., maximization of mutual inductance $M = 1/K_{A-\Phi}$ of the input coil and SQUID interferometer).

The experiments show that the best result with respect to coefficient $K_{A-\Phi}$ is obtained for spiral coils with 20 turns, an inner hole diameter of $d = 0.35 \text{ mm}$, and an outer hole diameter of $D = 2 \text{ mm}$. At an induc-

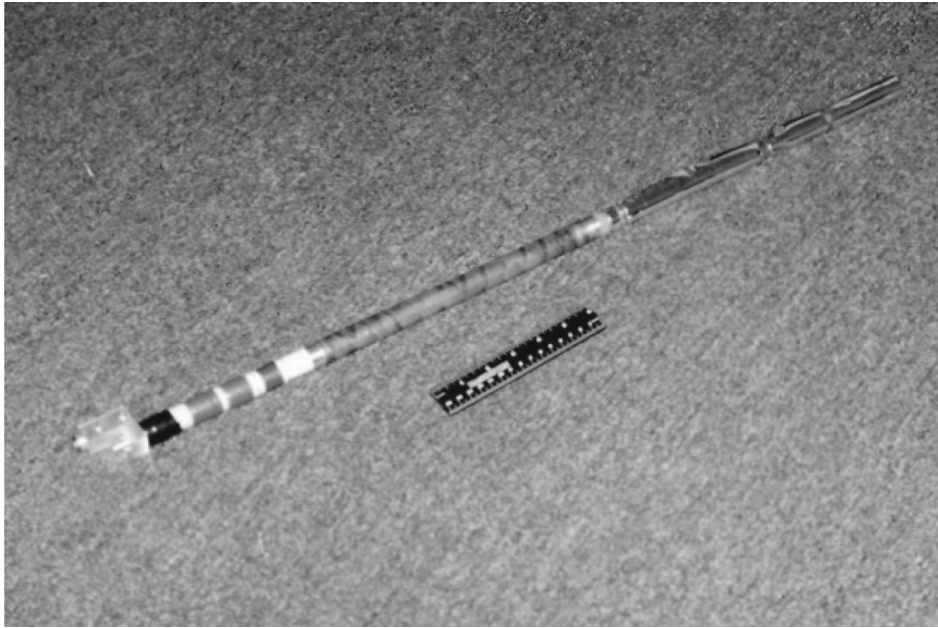


Fig. 3. Photograph of the measurement probe of the single-channel SQUID gradiometer with mechanical balancing of the signal gradiometer. The intrinsic noise of the SQUID magnetometer is estimated to be $12\text{--}18 \text{ fT/Hz}^{1/2}$.

tance of $L_{\text{hc}} \approx 0.8 \text{ } \mu\text{H}$, coefficient $K_{A-\Phi}$ is about $0.8 \text{ } \mu\text{A}/\Phi_0$.

The mutual inductance of the input coil and SQUID for the above hybrid sensor ($M \sim 2.5 \text{ nH}$) is comparable with the inductance ($M = 2.6 \text{ nH}$) of a SUPRACON AG CCblue fully integrated SQUID sensor, in which the spiral input coil is fabricated using the thin-film technology on top of the SQUID interferometer.

1.2. Measurement Probe of the Prototype of Single-Channel SQUID Gradiometer

The measurement probe of the prototype of SQUID gradiometer (Fig. 3) is based on fibreglass tubes and consists of the following elements: (i) transformer of magnetic flux representing a second-order axial gradiometer, (ii) SQUID sensor with the dc-current SQUID and input coil, (iii) superconducting balancers for mechanical balancing of gradiometer in the presence of uniform magnetic field, (iv) upper cover with balancing screws, electric socket, and fitting for liquid helium.

The second-order gradiometer is made of insulated niobium wire with a diameter of 0.1 mm using the $2 : 4 : 2$ configuration (two lower, four central, and two upper turns) on a graphite substrate with a diameter of 16 mm . The diameter of the receiving turns of the gradiometer is 15.8 mm and the size of the base is 55 mm . The initial unbalance is no greater than 0.1% . The gradiometer ends are mechanically fixed on niobium lamellas of the SQUID sensor for the connection to the SQUID input coil.

For operation in the absence of magnetic shielding, the gradiometer is equipped with additional system for mechanical balancing in the presence of uniform magnetic field based on superconducting balancers that can be shifted in the region of the receiving loops of gradiometer with the aid of dielectric links and screws. The mechanical balancing makes it possible to decrease the unbalance of gradiometer to less than 0.01% . The balancing of gradiometer is performed using the procedure that is similar to the procedure of [11]. The difference lies in the fact that the minimization of the test signal of the uniform magnetic field at the output of the SQUID gradiometer that is generated by the Helmholtz coils along the X , Y , and Z directions is performed using the mechanical displacement of the corresponding superconducting balancer.

In the tests of the gradiometer in such a configuration, we experimentally obtain the coefficient of conversion of input magnetic field B_{in} into SQUID magnetic flux Φ_{hc} ($4\text{--}6 \text{ nT}/\Phi_0$) that corresponds to an equivalent sensitivity of gradiometer with respect to magnetic field of $12\text{--}18 \text{ fT/Hz}^{1/2}$ at a SQUID intrinsic noise of about $3 \text{ } \mu\Phi_0/\text{Hz}^{1/2}$. Such a sensitivity is sufficient for application of SQUID gradiometers in the NDT systems.

1.3. Electronics and Control Unit of the Prototype of Single-Channel SQUID Gradiometer

SQUID electronics of the prototype of the magnetometric system is mounted on an aluminum unit with sizes of $157 \times 82 \times 17 \text{ mm}$ (Fig. 4), located in the vicin-



Fig. 4. Photograph of the SQUID electronics and control unit of the prototype of the single-channel SQUID gradiometer.

ity of the cryostat, and connected to the measurement probe using a cable with a length of 70 cm. The SQUID electronic system contains analog and digital circuits. The analog part contains the conventional modulation circuit of null detector and the circuit of negative feedback with respect to magnetic flux. The analog circuit provides the tuning of the SQUID working parameters. The digital circuit make it possible to switch the tuning and working regimes of the SQUID gradiometer and control the system using a PC. The SQUID electronics is connected to the control unit with the aid of a 5-m-long cable.

The preamplifier of the electronic unit is based on a Toshiba K-369 low-noise FET in the cascade circuit. The intrinsic noise of the preamplifier is no greater than $0.7 \text{ nV/Hz}^{1/2}$.

A single-pole integrator generates the feedback signal that is fed to the modulation coil via a feedback resistor. The voltage across the feedback resistor is used as the output signal of magnetometer. The electronic system works at a fixed feedback coefficient of about $2 \text{ V}/\Phi_0$. The gain of the electronic system is about -3 dB in a frequency interval of $0\text{--}16 \text{ kHz}$ when the feedback circuit is closed and the input signal is equivalent to $0.1 \Phi_0$ in the SQUID.

The control unit of the magnetometric system contains stabilized power supply sources, additional amplifier of the input signal, and circuits of micropro-

cessor control that are used for tuning and switching of working regimes of the SQUID system.

The working regimes of the prototype of the SQUID system are controlled using codes that are generated by digital circuits of the control unit when the corresponding buttons are pressed in the main window of the control software on the monitor. The output signal of the magnetometer is fed to the oscilloscope or spectrum-analyzer input for the further analysis. The front panel of the unit also accommodates a connector via which the test signal from the output of the audio-frequency generator can be delivered in the course of tuning of the SQUID working parameters.

1.4. Fiberglass Cryostat of the Prototype of Single-Channel SQUID Gradiometer

Figure 5 presents the photograph of the helium cryostat of the prototype of single-channel SQUID gradiometer.

The inner diameter of the neck and tail of the cryostat is 17 mm. The distance between the outer and inner surfaces in the tail in the cooled system is no greater than 6 mm. The working time of liquid helium (1.2 L) in the cryostat is about 2 days. The cryostat parameters are as follows: outer diameter, 110 mm; length, 500 mm; outer diameter of the tail, 45 mm; outer length of the tail, 230 mm; inner diameter of the neck, 17 mm; inner diameter of the cryogenic flask,

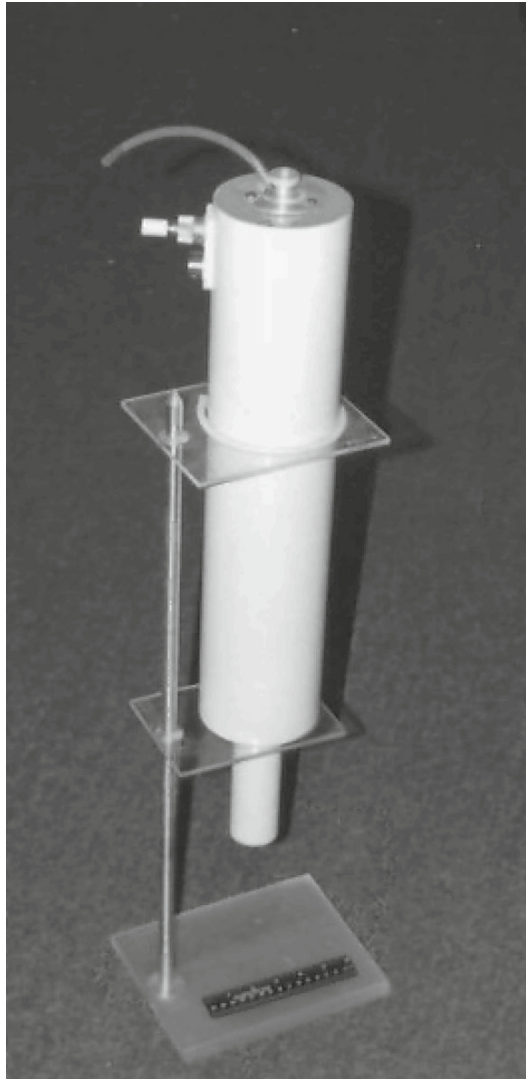


Fig. 5. Photograph of the fiberglass helium cryostat of the prototype of SQUID gradiometer.

80 mm; diameter of the inner tail, 17 mm; inner length of the tail, 290 mm; heat–cold distance, 6 mm; volume of liquid helium, 1.2 L; time of the total evaporation of liquid helium, 48 h; and weight of empty cryostat, 1.2 kg.

The cryostat volume is relatively small, so that the filling procedure is relatively simple and takes several minutes. The small volume of helium and the presence of safety valve provide the safety of cryostat when vacuum conditions in the space between the inner and outer walls are violated.

2. EXPERIMENTAL RESULTS

The above elements are used to construct a working prototype of the SQUID gradiometer. The prototype is practically tested under laboratory conditions and the main working parameters are studied. A Stanford

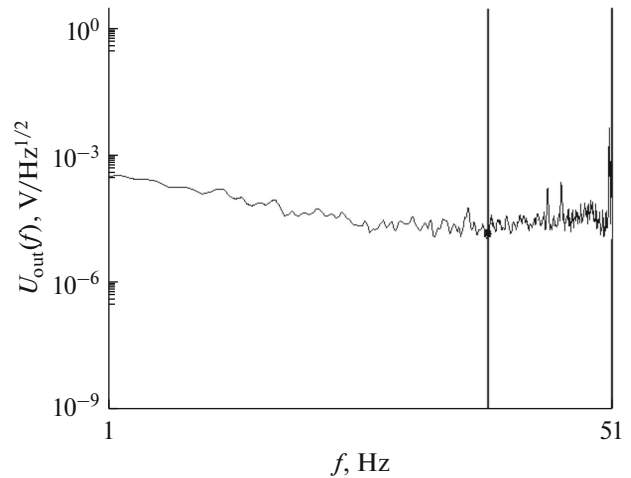


Fig. 6. Noise spectrum of output voltage of SQUID gradiometer $U_{\text{out}}(f)$ measured under laboratory conditions in the absence of additional magnetic shielding. The cursor position corresponds to a frequency of $f = 19.4$ Hz and a noise spectral density of the output voltage of $U_{\text{out}} = 11.44 \mu\text{V}/\text{Hz}^{1/2}$.

Research low-frequency spectrum analyzer is used to study the noise characteristics of the output signal of the prototype of SQUID gradiometer. Figure 6 presents a typical noise spectrum of the output voltage of SQUID gradiometer that is measured at the center of Moscow.

The noise spectra are measured in a frequency interval of 1–50 Hz. A noise spectral density of 11–12 $\mu\text{V}/\text{Hz}^{1/2}$ measured at a feedback coefficient of $K_{\text{FB}} = 2 \text{ V}/\Phi_0$ and coefficient $K_{\text{A-}\Phi}$ of the conversion of magnetic field into the SQUID magnetic flux of about $5 \text{ nT}/\Phi_0$ corresponds to an equivalent noise with respect to magnetic field of about $30 \text{ fT}/\text{Hz}^{1/2}$. Such noise levels of the SQUID gradiometer indicate sufficient balancing and prove that such devices can be employed in the NDT systems. The SQUID gradiometers can be used to develop multichannel SQUID systems but, in this case, the electronic balancing must be preferred to mechanical balancing.

CONCLUSIONS

The proposed prototype of the dc-current single-channel SQUID gradiometer exhibits stable operation under laboratory conditions in the absence of additional magnetic shielding and can be used for the development of a multichannel magnetometric SQUID system for NDT of defects in metal structures and materials.

The experimental results show that a fully integrated SQUID sensor must be developed, since the application of the thin-film input coil of the transformer of magnetic flux in the SQUID will make it

possible to increase the coupling coefficient of the input coil and SQUID inductance by a factor of greater than 2. Thus, the resulting sensitivity of the SQUID gradiometer can also be increased by a factor of greater than 2. The topology of the SQUID interferometer must have the gradiometer structure to suppress the direct effect of external magnetic fields including the magnetic biases that excite eddy currents in the samples under study. Such an approach will make it possible to substantially simplify the structure of the superconducting shields of the SQUID sensor.

ACKNOWLEDGMENTS

This work was supported by the Russian Science Foundation (project no. 15-19-00206).

REFERENCES

1. G. B. Donaldson, A. Cochran, and D. A. McKirdy, *SQUID Sensors: Fundamentals, Fabrication and Applications*, Ed. by H. Weinstock (Kluwer, Dordrecht, 1996).
2. H.-J. Krause and M. Kreuzbruck, *Physica A* **368** (1), 70 (2002).
3. R. J. P. Bain, G. B. Donaldson, S. Evanson, and G. Hayward, *IEEE Trans. Magn.* **23**, 473 (1987).
4. H. Weinstock and M. Nisenoff, in *Proc. 3rd Int. Conf. on Superconducting Quantum Interference Devices and Their Applications (SQUID'85), Berlin (West), June 25–28, 1985*, Ed. by H. D. Hahlbohm and H. Lubbig, (De Gruyter, Berlin, 1985), p. 843.
5. G. Sawade, J. Straub, H. J. Krause, et al., in *Proc. Int. Symp. on Non Destructive Testing in Civil Engineering (NDTCE), Berlin, 1995* (DGZfP, Berlin, 1995).
6. Y. Tavrín, M. Siegel, and J.-H. Hinken, *IEEE Trans. Appl. Supercond.* **9**, 3809 (1999).
7. V. P. Koshelets, A. N. Matlashov, I. L. Serpuchenko, et al., *IEEE Trans. Magn.* **25**, 1182 (1989).
8. A. N. Matlashov, V. P. Koshelets, Yu. E. Zhuravlev, et al., *IEEE Trans. Magn.* **27**, 2963 (1991).
9. L. V. Filippenko, S. V. Shitov, P. N. Dmitriev, et al., *IEEE Trans. Appl. Supercond.* **11**, 816 (2001).
10. J. Jaycox and M. Ketchen, *IEEE Trans. Magn.* **17**, 400 (1981).
11. Yu. V. Maslennikov, *J. Commun. Technol. Electron.* **56**, 991 (2011).

Translated by A. Chikishev